Identifying Electric Shock in the Human Body via α Dispersion

Heng Zhao, Xianyong Xiao, *Senior Member, IEEE*, and Qiuqin Sun, *Member, IEEE*

***Abstract*—The ability to identify electric shock in the human body is a crucial consideration in the design of touch/leakage protective devices. In this paper, the α-dispersion characteristics of electrical impedance in the human body are investigated based on the Cole–Cole model. An improved electric shock identification method is proposed accordingly. The effects of various factors (e.g., transition resistance and feeder reactance) on the accuracy and reliability are analyzed. Feasibility and effectiveness of the method are verified via numerical simulation. The results indicate that 1) α-dispersion is an effective feature for distinguishing living or non-living organisms; 2) the proposed method is robust and unaffected by transition resistance; and 3) the computational cost is low to satisfy standard leakage current protective device requirements. This paper provides a solution to the dead-zone problem as well as a set of workable guidelines for protective device design.**

***Index Terms*—Human body shock, feature extraction, human body impedance, Cole-Cole model, α-dispersion.**

I. Introduction

TOUCH and leakage electrical accidents occur in rural areas frequently due to the lack of safety awareness, poor quality of power equipment, complexities of meteorology, and other complex factors. Techniques for identifying electric shock characteristics in the human body successfully are invaluable for saving lives.

Residual current devices (RCDs) are commonly employed in rural areas and distribution networks to guarantee reliability in power supplies [1]. RCDs perform touch/leakage protection through a three-level-protection strategy. Total protection, branch protection, and terminal protection. Theoretically, by considering both naturally leakage current and power supply reliability, the thresholds are set to 100–500 mA and 0.2–0.5 s for three-phase total protection, 50–100 mA and 0.1–0.2 s for single-phase branch protection, and 15–30 mA and 0 s for single-phase terminal protection, respectively. In practice, however, the natural leakage current is affected by many factors, such as the environmental and load conditions. There are few efficient methods available to identify leakage current or touch accidents, or to classify the shock characteristics between a living body and a non-living body.

Extensive research has been conducted to address this issue [2]–[5]. Reference [2] proposed a protection scheme that exploits residual current information along with abrupt changes in leakage current. Reference [3] proposed an adaptive method considering environmental conditions and natural leakage current. Based on field measurement, an adaptive neural network was employed by [4], [5] to detect shock current and identify failure modes. None of these techniques take detailed electric shock characteristics into account. Further more, the threshold is lower than 30 mA which is quite small [6]. It is difficult to identify electric shock accurately via amounts of leak currents and its variations only. Comprehensive and highly accurate electric shock characteristics for human bodies are required.

The Cole-Cole theory and bioimpedance dispersion characteristics can elucidate the differences in electrical impedance between living bodies and non-living bodies clearly [7]–[12]. The α-dispersion characteristics of electrical impedance in human bodies were investigated in this study based on the Cole-Cole model. An electrical impedance parametric method was proposed to identify electric shock characteristics in human bodies accurately, and the impact of transition resistance on the accuracy of the proposed method was determined. The feasibility and effectiveness of the proposed method were also verified through numerical simulations.

II. Human Body Impedance Model and Electric Shock Characteristics

A. Ideal Model of Human Tissue

The human body consists of cells bathed in extracellular fluid. The equivalent circuit of a human cell is shown in Fig. 1(a).

R_m, R_i and R_e represent the resistors; C_m, C_i and C_e represent the capacitors. C_e and C_i are quite small whereas R_m is relatively large [13], so the current can be simplified using two resistors and one capacitor in parallel as shown in Fig. 1(b). The human body has high resistance to low-frequency current and low resistance to high-frequency current [14]. Classic three-component impedance models include the Fricke biological tissue model and IEC body impedance model which are shown in Fig. 2(a) and (b) respectively.

Manuscript received January 2, 2017; revised June 30, 2017; accepted October 14, 2017. Date of publication October 26, 2017; date of current version April 6, 2018. This work was supported by the State Grid Corporation of China under Grant SGSCZG00YJKJ1313422. Paper no. TPWRD-00003-2017. *(Corresponding author: Heng Zhao.)*

H. Zhao and X. Xiao are with the College of Electrical Engineering and Information Technology, Sichuan University, Chengdu 610055, China (e-mail: 32820160@qq.com; xiaoxianyong@163.com).

Q. Sun is with the Department of Electrical Engineering, Hunan University, Changsha 410082, China (e-mail: sunqq@hnu.edu.cn).

Color versions of one or more of the figures in this paper are available online at http://ieeexplore.ieee.org.

Digital Object Identifier 10.1109/TPWRD.2017.2766169

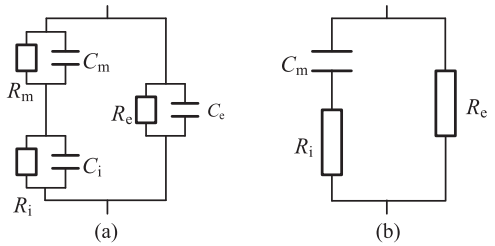

Fig. 1. Equivalent circuit models of a human cell: (a) an ideal model and (b) a simplified ideal model.

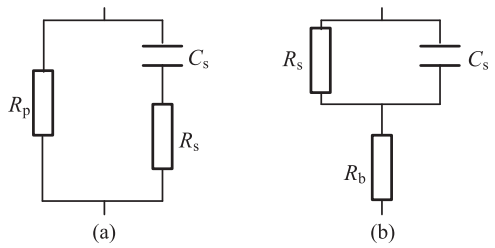

Fig. 2. Three-component model of human tissues: (a) Fricke model and (b) IEC model.

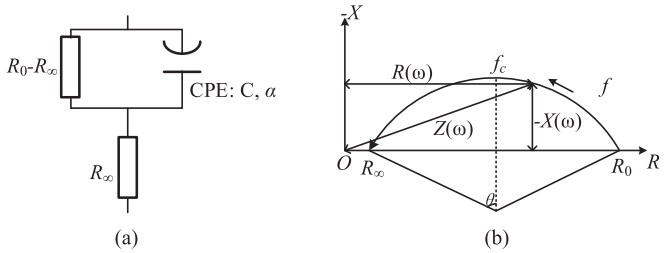

Fig. 3. (a) The Cole-Cole resistance model and (b) its complex plane plot.

B. Cole-Cole Model of Human Tissue

The equivalent impedance of IEC model is expressed in Fig. 2(b).

$$Z(\omega) = R_b + \frac{R_s}{1 + j\omega C_s R_s} \tag{1}$$

In the complex impedance plane, $Z(\omega)$ is the upper half of a circle centered at the horizontal axis. Its two points intersecting the axis are $R_b + R_s$ (for $\omega = 0$) and R_b (for $\omega = \infty$), where ω is the angular frequency; R_b and R_s are the resistances of the body and skin, respectively. C_s is the capacitance of skin. The resistance and capacitance of human body impedance circuits vary with frequency, i.e., the human equivalent impedances are different. The circle center for the arc $Z(\omega)$ is below the real axis. Cole proposed the impedance model shown in Fig. 3(a) based on the results of a series of experiments.

The model can be expressed as follows [11]

$$Z(\omega) = R_\infty + \frac{R_0 - R_\infty}{1 + (j\omega\tau)^\alpha} \tag{2}$$

where R_∞ and R_0 are the resistances for high frequency and low frequency, respectively, τ is a time constant which is determined by the characteristic frequency as $f_c = \pi\tau/2$, it is the frequency corresponding to the highest point of the impedance semicircle. The term α is the coefficient related to the dispersion characteristics. Mathematically, $\alpha = 2\theta/\pi$ within the range of $[0, 1]$. The center is determined by α, it is located on the axis with the impedance described by (1). The circle center is below the real axis for $\alpha < 1$ and has impedance that can be modeled by (2). In the Cole-Cole impedance model, a constant phase element (CPE) is used to replace the ideal capacitive element C_s.

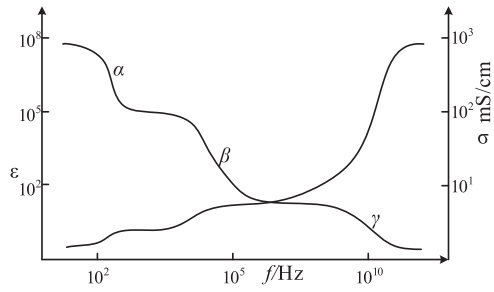

Fig. 4. Frequency characteristics of biological tissue dielectric constant ε and conductivity σ versus frequency.

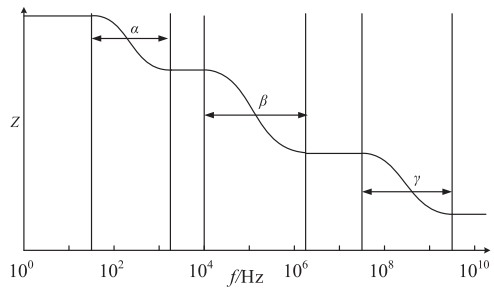

Fig. 5. Hypothetical frequency impedance diagram of biological tissue.

As we know

$$j^a = \cos\left(\frac{\alpha\pi}{2}\right) + j\sin\left(\frac{\alpha\pi}{2}\right) \tag{3}$$

we obtain

$$R(\omega) = R_\infty + \frac{(R_0 - R_\infty)\left[1 + (\omega\tau)^\alpha \cos\left(\frac{\alpha\pi}{2}\right)\right]}{1 + 2(\omega\tau)^\alpha \cos\left(\frac{\alpha\pi}{2}\right) + (\omega\tau)^{2\alpha}} \tag{4}$$

$$X(\omega) = -\frac{(R_0 - R_\infty)(\omega\tau)^\alpha \sin\left(\frac{\alpha\pi}{2}\right)}{1 + 2(\omega\tau)^\alpha \cos\left(\frac{\alpha\pi}{2}\right) + (\omega\tau)^{2\alpha}} \tag{5}$$

C. Human Body Electric Shock Characteristics

In 1957, Schwan *et al.* discovered the bioimpedance dispersion phenomenon [12] which can be classified as α-dispersion, β-dispersion, and γ-dispersion [16], [17]. These three types of dispersion correspond to audio frequency (Hz to kHz), radio frequency (kHz to MHz), and microwave frequency (MHz to GHz), respectively. The biological tissue dielectric constant ε and electrical conductivity σ significantly vary in the different frequency range, as shown in Fig. 4. The bioimpedance within each dispersion range can be described by the Cole-Cole

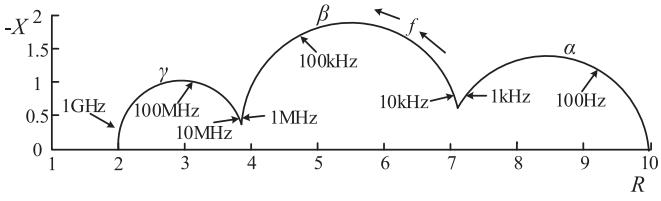

Fig. 6. Hypothetical Cole-Cole impedance plot of biological tissue showing the 3 overlapping dispersions of α, β and γ ranges.

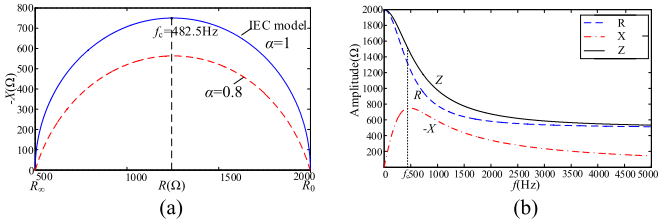

Fig. 7. (a) Impedance locus of human body impedance. (b) Impedance vs. frequency for IEC model.

equation, as illustrated in Fig. 5. When the three types of dispersions simultaneously exist, they overlap as shown in Fig. 6 [17].

The power system examined here contains harmonics with frequencies ranging from tens of Hz to kHz, which belong to the α-dispersion class. Therefore, α-dispersion can be used to identify electric shock in the human body.

III. Characteristics of Electric Shock

The electric shock characteristics of human bodies are well in accordance with the dispersion theory proposed by Schwan. Out of all the components of the human body, the equivalent impedance is mainly determined by the skin [6]. Experiments have shown that the longer the time spent in vitro, the weaker the dispersion characteristics [18]. In other words, the dispersion characteristics of fresh tissue are more obvious than those of older tissue. The dispersion coefficients of non-living objects are about 1 [11], while the dispersion coefficients of human bodies are far less than 1. Hence, the equivalent impedance model satisfies both the dispersion theory and Cole-Cole theory. The Cole-Cole equation can be used to describe electric shock behavior [16]–[20] and the dispersion coefficient can be used for feature extraction.

The IEC model shown in Fig. 2(b), with $R_s = 1500\ \Omega$, $C_s = 0.22\ \mu$ F and $R_b = 500\ \Omega$ [15], is an ideal model. In a special case where $\alpha = 1$, and other Cole-Cole terms are $\tau = R_s C_s = 0.33$ ms, $f_c = 1/2\pi\tau = 482.3$ Hz, $R_0 = R_b + R_s$ and $R_\infty = R_b$. The resulting impedance circle is shown as a solid line in Fig. 7(a). Fig. 7(b) shows the real and imaginary parts of the impedance vary with frequency. However, this model is mainly applied to fundamental frequency, and it is difficult to distinguish human-body electric shock from other electric shocks. Our proposed model starts with α-dispersion characteristics to establish a constant phase element (CPE: Cs,α) contained human body impedance model, as shown in Fig. 8(a).

Again, human body impedance is mainly determined by skin impedance, and the value of α for human skin is about 0.8 [20].

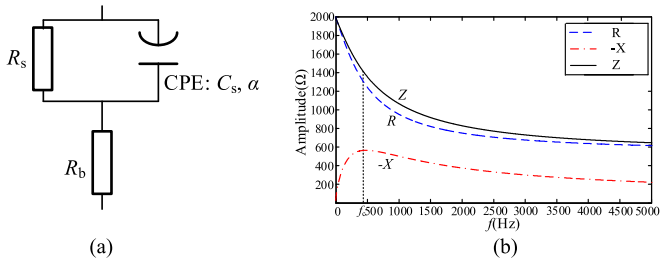

Fig. 8. (a) Human body impedance model considering α-dispersion. (b) Impedance vs. frequency for α-model.

Thus, the value of α for the human body can be assumed to be 0.8. The human body impedance circle diagram with dispersion characteristics is marked with a dotted arc in Fig. 7(a). The real part and imaginary parts of impedance varying with frequency are shown in Fig. 8(b).

IV. Method for Identifying Human Body Electric Shock

According to the Cole-Cole theory, biological tissue impedance is determined by four parameters: R_0, R_∞, τ and α. As shown in Fig. 3(b), if three or more complex impedance values for different frequencies can be measured, then the impedance semicircle parameters and Cole-Cole parameters can be estimated. Because power grids inevitably contain harmonics [16], when a human body is suffering an electric shock, the parameters of biological tissue can be estimated by the harmonic content, i.e., the Fourier transform (FFT). The complex impedance can be obtained by dividing the corresponding angular frequencies. If naturally leakage current is non-negligible, each residual current should be the variation from before to after the shock.

Assume that N complex impedance points are measured, i.e., (R_1, X_1), (R_2, X_2), $\cdots$, (R_N, X_N), which satisfy the impedance semicircle shown in Fig. 3(b). The circle is centered at (a, b) and has a radius of R.

The distance from any impedance point to the circle center, D_n, satisfies the following:

$$D_n^2 = (R_n - a)^2 + (X_n - b)^2. \tag{6}$$

The goal is to find the optimal a and b to minimize the variance of D_n

$$\mathrm{Var}(D_n^2) = \frac{1}{N}\sum_{i=1}^{n}\left[D_n^2 - \frac{1}{N}\sum_{m=1}^{n} D_m^2\right]^2. \tag{7}$$

By setting the partial derivatives of a and b to zeros, we can obtain the circle center by solving the following:

$$\begin{pmatrix} a \\ b \end{pmatrix} = \begin{pmatrix} 2\sum_{n=1}^{n} R_{cn}^2 & 2\sum_{n=1}^{n} R_{cn}X_{cn} \\ 2\sum_{n=1}^{n} R_{cn}X_{cn} & 2\sum_{n=1}^{n} X_{cn}^2 \end{pmatrix}^{-1} \times \begin{pmatrix} \sum_{n=1}^{n}(R_{2cn} + X_{2cn})R_{cn} \\ \sum_{n=1}^{n}(R_{2cn} + X_{2cn})R_{cn} \end{pmatrix} \tag{8}$$

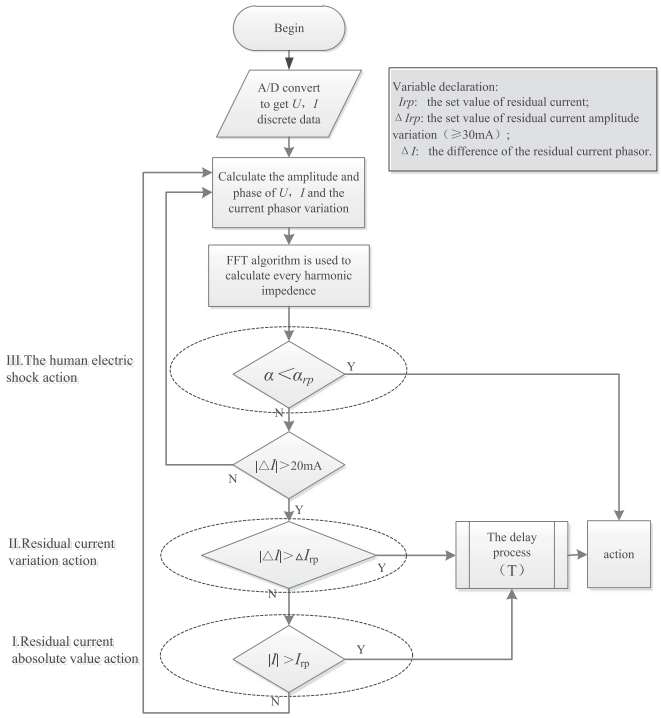

Fig. 9. Flowchart for the identification of electric shock.

Where

$$R_{cn} = R_n - \frac{1}{N}\sum_{n=1}^{n} R_n \tag{9}$$

$$R_{2cn} = R_n^2 - \frac{1}{N}\sum_{n=1}^{n} R_n^2 \tag{10}$$

$$X_{cn} = X_n - \frac{1}{N}\sum_{n=1}^{n} X_n \tag{11}$$

$$X_{2cn} = X_n^2 - \frac{1}{N}\sum_{n=1}^{n} X_n^2 \tag{12}$$

The radius of the circle is

$$R = \frac{1}{N}\sum_{n=1}^{n} D_n \tag{13}$$

The parameters, i.e. R_0, R_∞, τ and α, are computed by

$$R_\infty = a - \sqrt{R^2 - b^2} \tag{14}$$

$$R_0 = a + \sqrt{R^2 - b^2} \tag{15}$$

$$\alpha = \frac{2}{\pi}\arccos\frac{b}{R} \tag{16}$$

$$\tau = \frac{\left[\frac{R_0 - R_\infty}{Z(\omega) - R_\infty} - 1\right]^{\frac{1}{\alpha}}}{j\omega} \tag{17}$$

Once the dispersion coefficient is lower than the threshold, an electric shock accident can be identified. This electric shock identification procedure, as shown in Fig. 9, includes three steps:

TABLE I
HARMONIC MEASURED FROM AN OFFICE BUILDING

Harmonic Order	U(V)	Harmonic Order	U(V)
DC	0.02	6	0.01
1	233.23	7	4.56
2	0.40	8	0.10
3	1.20	9	0.64
4	0.40	10	0.09
5	2.09	11	1.20

1) detecting steady-state residual current, 2) detecting mutational residual current, and 3) identifying the electric shock. Each step comes with a different strategy.

Step (I): Alarms, long-delay actions, or other signals are used to mark gradual variations in residual current caused by environmental changes, line aging, load changes, and so on.

Step (II): For normal leakage, short-delay actions are employed by prejudging whether electric shock exists by detecting current mutations.

Step (III): Electric shock in human bodies must be identified as rapidly and accurately as possible. Once such an electric shock is identified, no delay strategy is involved, otherwise, action will follow step (I) or (II).

The priorities of the three steps are (III) > (II) > (I) to maintain the advantages of existing protection methods while better protecting human bodies from electric shock.

V. RESULTS AND DISCUSSION

A. Simulation Study

The electric shock model explored here was established in PSCAD with the following parameters: 4 Ω grounding impedance of voltage sources, $R_p = 50$ kΩ normal line leakage impedance, and $C_p = 0.07$ μF. With the IEC model [15], we verified the adaptability of the proposed method by varying the R and C values. The voltage source contains harmonics, its parameters were obtained from measured data for an average office building [13], as shown in Table I. We selected the waves with higher contents including the 1th, 3th, 5th, 7th, 9th and 11th-order harmonics as shown Table I to calculate α and other parameters. The simulation results, as shown in Table II, indicated that the relative error of α was less than 0.17%. This indicated that the Cole-Cole impedance parameters can be accurately identified using the proposed model.

B. Influence of Transition Resistance

We varied the transition resistance values to determine their effects on the results obtained via the model presented in Section V-A. As reported in Table III, the term R_t is the transition resistance (including contact resistance, resistance to ground, line resistance, and other factors). Transition resistance has little influence on the measurement of α. In model 5 of Table III, the touch resistance was 10 000 Ω, the RMS fault current was 18.83 mA, and at the time, the calculation error

TABLE II
RESULTS FOR PARAMETER ESTIMATION

Model	$R_b(\Omega)$	$R_s(\Omega)$	$C_s(\mu F)$	Theoretical Value Of Parameters			Estimation Value Of Parameters			Error
				$R_0(\Omega)$	$R_\infty(\Omega)$	α	$R_0(\Omega)$	$R_\infty(\Omega)$	α	$\alpha\%$
1	500	1500	0.22	2000	500	1	1998.45	498.67	0.9999	0.01
2	800	1000	0.11	1800	800	1	1797.85	800.95	0.9961	0.39
3	500	1000	0.22	1500	500	1	1502.24	504.56	0.9984	0.16
4	1200	1000	0.33	2200	1200	1	2200.33	1200.4	0.9991	0.09
5	800	1600	0.22	2400	800	1	2398.51	813.82	0.9982	0.18

TABLE III
IMPACT OF TRANSITION RESISTANCE ON PARAMETER ESTIMATION

Mode	$R_t(\Omega)$	$I_f(mA)$	$R_0(\Omega)$	$R_\infty(\Omega)$	α	$\alpha\%$
1	50	114.13	2049.4	550.61	0.9872	1.28
2	500	101.27	2300.1	1274.03	0.9928	0.72
3	2000	66.64	3499.91	2497.64	0.9997	0.03
4	6000	28.46	8199.92	7200.97	0.9999	0.01
5	10 000	18.83	12400.56	10793.56	0.9978	0.22

TABLE IV
IMPACT OF FEEDER REACTANCE ON PARAMETER ESTIMATION

Line Length(m)	$L_l(\Omega)$	$R_l(H)$	$R_0(\Omega)$	$R_\infty(\Omega)$	α	$f_c(Hz)$
10	6.6810-5	0.04	2000.1	499.7	0.7998	482.55
50	3.3410-4	0.2	2000.0	503.9	0.8004	480.63
100	6.6810-4	0.4	2000.2	507.0	0.8005	479.51
500	3.3410-3	2	2001.5	530.9	0.8013	470.56
1000	6.6810-3	4	2003.3	559.9	0.8021	459.70

was found to be 0.22%. A larger touch resistance did not impact the accuracy of calculated results. Consideration of greater touch resistance was not required, because a fault current below 30 mA will ensure human safety. Theoretically, the transition resistance is equivalent to superimposing R_t to the original R_b, and only affects R_0 and R_∞ , in other words, it only alters the horizontal position of the impedance semicircle without affecting the shape or size of the circle. Therefore, α is maintained constant.

C. Influence of Other Parameters

In practice, the line leakage impedance may contain parallel distributed capacitance and series inductance. We performed simulation and comparisons of the proposed human-body impedance model (i.e., the series/parallel network model including capacitors or leakage impedance or transition impedance of the inductance) in MATLAB. In the human body impedance model, we set $\alpha = 0.8$ and fixed the values of the other parameters: $f_c = 482.3$ Hz, $R_0 = 2000\,\Omega$ and $R_\infty = 500\,\Omega$. Parameters for a real line were set to $r = 0.004\,\Omega$/m, $l = 6.68 \times 10^{-6}$H/m, and the leakage impedance was set per the relevant standards. The results are shown in Tables IV and V. In Table V, R_p and C_p are the leakage resistance and the leakage capacitance, respectively. Term Z_p is the leakage impedance, and I_l is the RMS of the leakage current.

TABLE V
IMPACT OF FEEDER LEAKAGE IMPEDANCE ON PARAMETER ESTIMATION

Mode	$R_p(k\Omega)$	$C_p(\mu F)$	$Z_p(k\Omega)$	$I_l(mA)$	$R_0(\Omega)$	$R_\infty(\Omega)$	α	$f_c(Hz)$
1	80	0	80	2.75	1951.8	490.2	0.7979	497.4
2	160	0.02	113.1	1.95	1975.1	354.1	0.8142	472.7
3	$+\infty$	0.04	79.6	2.76	1999.5	254.1	0.8278	437.7
4	160	0.04	71.3	3.09	1974.7	253.7	0.8279	443.5
5	80	0.03	63.9	3.44	1950.9	298.7	0.8212	464.9
6	50	0.04	42.3	5.2	1922.6	253.2	0.8279	456.0

As shown in Table IV, even if the transition impedance contains relatively small reactance (typically no more than 500 m for a low-voltage line), the obtained value of α is significantly less than 1. Table V shows that the estimated value of α is still far less than 1 even when the normal leakage current is ignored during Cole-Cole impedance parameter estimation, because the normal leakage current is small for the actual line. Moreover, because the Cole-Cole impedance equation is an equivalent one which comprehensively considers all single-cell equivalent impedance [13], [14], the impact of non-principal components is limited when the dispersion coefficient of the principal component is significantly less than 1.

D. Comparison With Existing Methods

Modern devices typically use the residual current $|I_h|$ or its variation $\Delta|I_h|$ as the criterion. The current mode and current pulse mode protection are the representatives. The proposed method is compared here with other existing methods by appropriately combining different normal leakage impedance, touch/leakage fault impedance, transition resistance, and other parameters (Section V-C). In the simulations, the current and current pulse mode were assumed to be 50 mA and 30 mA, respectively. The safety threshold under which the protection system takes action was set to 30 mA. The results are shown in Table VI.

When the line is perfectly insulated ($I_l = 0$) and $I_f < 30$ mA, current mode, pulse mode, and the proposed method are correctly without actions in Mode 1. In Mode 6, only the proposed method can accurately identify shock and perform the actions. Similarly, in Modes 2 and 7, when $I_l = 0$ and $30 < I_f <$

TABLE VI
COMPARISON WITH EXISTING METHODS

Failure Mode		$I_l(mA)$	$I_f(mA)$	$I_k(mA)$	Current Movement Type $I_{n1}=50$ mA		Current Pulse Type $I_{n2}=30$ mA		The Method in This Paper			
					$\lvert I_k\rvert$	Movement	$\triangle\lvert I_k\rvert$	Movement	$I(\lvert I_k\rvert)$	$II\triangle\lvert I_k\rvert$	$III(\alpha)$	Movement
1		0.00	21.2	21.2	21.2	No	21.2	No	21.2	21.2	0.97	No, not human
2	Pure	0.00	40.3	40.3	40.3	**Refuse**	40.3	Yes	40.3	40.3	0.98	II move , not human
3	impedance	12.7	20.1	32.6	32.6	No	19.9	No	32.6	20.0	0.98	No, not human
4	leakage	16.8	40.3	43.7	43.7	**Refuse**	26.9	**Refuse**	43.7	40.3	1.00	II move, not human
5		25.4	28.0	52.6	52.6	**Mistake**	27.2	No	52.6	28.1	0.99	I move, not human
6	Human	0.00	20.9	20.9	20.9	**No**	20.9	**No**	20.9	20.9	0.82	III move, human
7	body	0.00	34.7	34.7	34.7	**Refuse**	34.7	Yes	34.7	34.7	0.79	II.III move, human
8	electric	14.5	20.9	31.2	31.2	**No**	16.7	**No**	31.2	21.0	0.83	III move, human
9	shock	18.7	38.4	49.5	49.5	**Refuse**	30.8	Yes	49.4	38.4	0.80	II.III move, human
10		28.9	36.4	53.3	53.3	Yes	24.4	**Refuse**	53.3	36.4	0.81	I.II.III move, human

The threshold value of step I and II for this method are set as 50mA and 30mA, whereas the threshold value of α for step III is set to be 0.9. I_l, I_f and I_k refer to natural leakage current, touch/leakage fault current and the total residual current.respectively. The parts of the table in bold indicates incorrect movement.

TABLE VII
HARDWARE SIMULATION RESULTS FOR ELECTROCUTION PHYSICS EXPERIMENTAL DATA

Test Object	$R_0(\Omega)$	$R_\infty(\Omega)$	α	Movability
IEC model	1799.8	501.9	0.9960	non-living being
Rabbit	2800.3	204.9	0.5335	living organism

50 mA, the pulse mode can perform correctly but the current mode does not. After the action of Step 2, the proposed method can identify the electric shock through the action of Step 3 in Mode 7.

When there is normal leakage current, the current mode acting on the total residual current can be either prevented from action (e.g., in Modes 4, 7, and 9), or wrongly put into action (e.g., in Mode 5). Because there are arbitrary phase relationships among I_l, I_f and I_h. The pulse mode acting on the variation of residual current may also refuse to act (e.g., in Modes 4 and 10). For example, in Mode 4, if the angle between I_l and I_f is obtuse and I_h is much smaller than the summation of I_l and I_f, both current mode and pulse mode fail to result in action. In Mode 5, if I_f is 28 mA, there should be no action but once I_h reaches 52.6 mA, the current mode acts wrongly. The proposed method can correctly recognize the current threshold via Step 1, and recognize that it is not human-body electric via Step 3, it can only alert or defer action to avoid power outages.

The current mode and pulse mode may wrongly act because protection settings cannot adjust in real time with the variation of naturally leakage current, touch/leakage fault current, and the phase relationship between the two currents. A protection dead zone and over-sensitive area exist, and the problem is fundamentally unsolvable even when the protection settings are adaptively adjusted. Our proposed method detects non-human-body electric shock by combining steady-state residual current and residual current mutations, thus reducing the protection dead zone and enhancing the accuracy of actions. Because the proposed method takes the dispersion coefficient α into account, the accuracy of identification is improved.

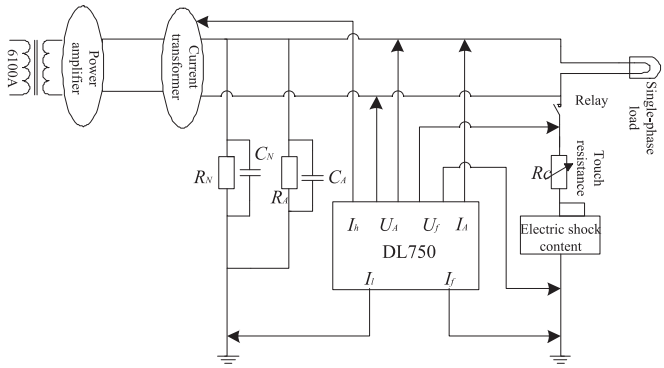

Fig. 10. Schematic diagram of Experiment.

E. Electric Shock Experiment

To validate the protection method proposed in this work, we established a physical electric shock test platform to measure the actual electric shock and leakage data. During this experiment, a FLUKE 6100 A standard disturbance source was used as the programmable power signal generator, a power amplifier was used to amplify the source signal to the voltage signal, and a YOKOGAWA DL750 oscilloscope was used to record the relevant voltage and current signal waveforms. In addition, three incandescent lamps with the following characteristics, 220 V, 50 Hz, 100 W were used to simulate the single-phase load, an iron shell capacitor, resistor, and sliding rheostat, were employed to simulate the circuit's insulation resistance and capacitance to ground. The schematic diagram of the experiment is shown in Fig. 10.

In Fig. 10, I_l, I_f and I_h represent the natural leakage current, touch/leakage fault current and total residual current, respectively, and U_f represents the fault branch voltage. When rabbits were used as the test subject, the contact sites were selected as the left forelimb and right hind limb, which were shaved to avoid the insulation imposed by the rabbits fur. It can be seen from the calculation results that the IEC model impedance circle center ordinate was approximately 0, and $\alpha = 0.996$, which was close to 1. By contrast, the rabbits produced an impedance semicircle

TABLE VIII
EXPERIMENTAL RESULTS OF IMPEDANCE ANALYZER

Experimental Subject	$R_0\,(\Omega)$	$R_\infty(\Omega)$	α
Human body (male)	8314.6	670.4	0.8627
Human body (female)	8302.4	417.0	0.8635
Fresh pork	4395.6	3324.1	0.6284
Pencil lead	125.0	124.9	1

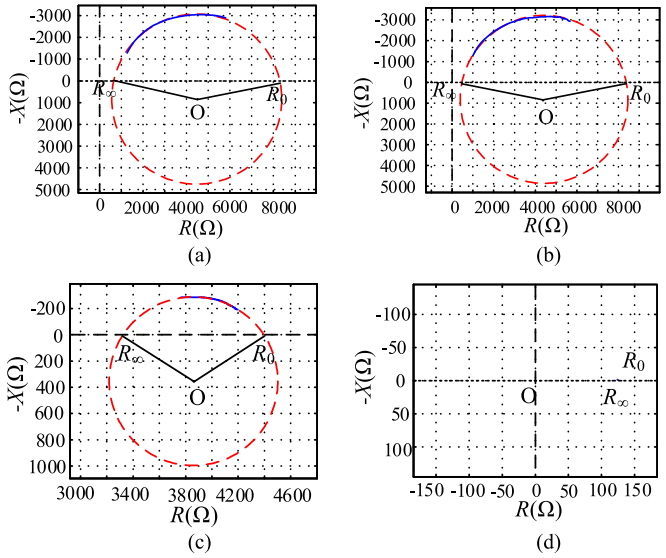

Fig. 11. Impedance charts for male, female, fresh pork and pencil lead.

whose center deviated down in comparison to the IEC model, and their $\alpha = 0.5335$, which was far less than 1.

Since electric shock tests conducted on humans are dangerous and contrary to ethical standards, we conducted a number of experiments using a IM3570 analyzer on a male and a female volunteer, fresh pork and pencil lead. A total of 801 points were scanned from 4 Hz to 5 kHz by selecting the constant voltage source mode (5 V). The results of the experiment are listed in Table VIII. The impedance chart was plotted for each test object using the measured data, as shown in Fig. 11. The α for human body and fresh pork were less than 1.

In terms of α, the value of α depends on many factors and is mainly determined by the skin tissue. Reference [19] examined the nonlinearity of human skin impedance under the Cole-Cole equation. Reference [14] tested α values between [0.68, 0.73]. Reference [20] tested α values between [0.79, 0.85]. In actual electric shock test, the α of rabbit was less than 1. In the impedance analyzer test, the α of human and fresh pork were also less than 1. These two experiments employing different theoretical approaches (actual electric shock test and impedance analyzer test) demonstrated that the dispersion characteristics in living organisms from different perspectives, which validated the effectiveness of the proposed method.

To evaluate the computational cost of the algorithm, the operation time for the entire process was 0.0156 s, plus the waiting time for two cycles of sampled signals, the total time consumption was 0.0556 s, which can meet the requirement that the operating time of protective device should be less than 0.1 s.

VI. CONCLUSION

In this paper, a novel method for human-body electric shock detection was proposed and tested to provide a basis for the design of touch/leakage protective devices. Our main conclusions can be summarized as follows.

1) Dispersion characteristics are the key to distinguish the electrical impedance of a living body and non-living body. The impedance of the human body falls under the frequency and scattering characteristics of the Cole-Cole theory.
2) The Cole-Cole impedance parameters can be estimated using the inherent harmonic constant of the distribution network and α-dispersion.
3) The α-dispersion coefficient is an effective feature for identifying human-body electric shock, protective devices can be improved by equipping them to detect the α-dispersion coefficient.
4) The effects of transition resistance and feeder reactance on α-dispersion are quite small. The computational cost of the proposed method meets standard application requirements.

ACKNOWLEDGMENT

The authors appreciate Prof. Yuquan Wei with Animal Center, Sichuan University, for providing the support of experiments.

REFERENCES

[1] M. Mitolo, "Shock hazard in the presence of protective residual-current devices," *IEEE Trans. Ind. Appl.*, vol. 46, no. 4, pp. 1552–1557, Jul./Aug. 2010.
[2] X. Luo, Y. Du, X. H. Wang, and M. L. Chen, "Tripping characteristics of residual current devices under nonsinusoidal currents," *IEEE Trans. Ind. Appl.*, vol. 47, no. 3, pp. 1515–1521, May/Jun. 2011.
[3] F. Freschi, "High-frequency behavior of residual current devices," *IEEE Trans. Power Del.*, vol. 27, no. 3, pp. 1629–1635, Jul. 2012.
[4] G. Cardoso, J. G. Rolim, and H. H. Zurn, "Application of neural-network modules to electric power system fault section estimation," *IEEE Trans. Power Del.*, vol. 19, no. 3, pp. 1034–1041, Jul. 2004.
[5] S. Czapp, "The impact of higher-order harmonics on tripping of residual current devices," in *Proc. 13th Int. Power Electron. Motion Control Conf.*, 2008, pp. 2082–2088.
[6] *Effects of current on human beings and livestock: Part 1 - General aspects*, IEC 60479-1. 2005.
[7] S. Wolny, "Aging degree evaluation for paper-oil insulation using the recovery voltage method," *IEEE Trans. Dielectr. Elect. Insul.*, vol. 22, no. 5, pp. 2455–2462, Oct. 2015.
[8] S. Wolny, A. Adamowicz, and M. Lepich, "Influence of temperature and moisture level in paper-oil insulation on the parameters of the cole-cole model," *IEEE Trans. Power Del.*, vol. 29, no. 1, pp. 246–250, Feb. 2014.
[9] S. Stoecklin, A. Yousaf, T. Volk, and L. Reindl, "Efficient wireless powering of biomedical sensor systems for multichannel brain implants," *IEEE Trans. Instrum. Meas.*, vol. 65, no. 4, pp. 754–764, Apr. 2016.
[10] T. J. Freeborn, B. Maundy, and A. S. Elwakil, "Extracting the parameters of the double-dispersion Cole bioimpedance model from magnitude response measurements,"*Med. Biol. Eng. Comput.*, vol. 52, no. 9, pp. 749–758, Jul. 2014.
[11] K. S. Cole, "Permeability and impermeability of cell membranes for ions," *Cold Spring Harbor Symp. Quant. Biol.*, vol. 8, pp. 110–122, Jan. 1940.
[12] H. P. Schwan and S. Takashima, "Electrical conduction and dielectric behavior in biological systems," *Encyclopedia Appl. Phys.*, vol. 5, pp. 177–200, 1993.

[13] M. Tang and C. Peng, "Bioimpedance measurement theory and technology," *J. Biomed. Eng.*, vol. 14, no. 2, pp. 152–175, Jun. 1997.
[14] L. De *et al.*, "Predicting body cell mass with bioimpedance by using theoretical methods: A technological review," *J. APPl. Physiol.*, vol. 82, no. 5, pp. 1542–1558, Dec. 1997.
[15] *Methods of Measurements of Touch Currents and Protective Conductor Current, Edition 2.0*, IEC 60990, 1999-2008.
[16] W. Kuang and S. O. Nelson, "Low-frequency dielectric properties of biological tissues: A review with some new insights," *Trans. ASAE*, vol. 41, no. 1, pp. 173–184, 1998.
[17] Damez *et al.*, "Dielectric behavior of beef meat in the 1-1500kHz range: Simulation with the Fricke/Cole-Cole model," *Meat Sci.*, vol. 77, no. 4, pp. 512–519, May 2007.
[18] H. P. Schwan, "Electrical properties of body tissues and impedance plethysmography," *IRE Trans. Med. Electron.*, vol. PGME-3, pp. 32–46, Nov. 1955.
[19] T. Yamamoto and Y. Yamamoto, "Non-linear electrical properties of skin in the low frequency range," *Med. Biol. Eng.*, vol. 19, no. 3, pp. 302–310, May 1980.
[20] E. A. White, M. E. Orazem, and A. L. Bunge, "Characterization of damaged skin by impedance spectroscopy: Mechanical damage," *Pharm. Res.*,vol. 30, no. 8, pp. 2036–2049, May 2013.

Heng Zhao received the B.S. and M.S. degrees from Chongqing University, Chonqing, China, and Sichuan University, Chengdu, China, in 2006 and 2012, respectively, both in electrical engineering. He is currently working toward the Ph.D. degree at Sichuan University. His research interests include electrical safety and power quality analysis.

Xianyong Xiao (SM'16) received the B.S., M.S., and Ph.D. degrees in electrical engineering and its automation from Sichuan University, Chengdu, China, in 1990, 1998, and 2010, respectively. Currently, he is a Professor in the College of Electrical Engineering and Information Technology at Sichuan University. He is interested in power quality, smart distribution systems, power system catastrophic events, uncertainty theory, and uncertain measures applied to power systems.

Qiuqin Sun (M'14) received the B.S. degree in electrical engineering from Chongqing University, Chonqing, China, in 2006, and the Ph.D. degree in electrical engineering from Shandong University, Jinan, China, in 2012. He is currently an Assistant Professor with Hunan University, Changsha, China. His research interests include electromagnetic transients and high-voltage engineering.